Inorganica Chimica Acta 556 (2023) 121623

Contents lists available at ScienceDirect

Inorganica Chimica Acta

journal homepage: www.elsevier.com/locate/ica

Cu(I) and Ag(I) complexes of two sterically demanding Xylyl-Substituted phosphine Ligands: Synthesis, Characterization, and structural examination

Manuel Vaz [a], Alberto Gobbo [b], M. Trinidad Martín [c], Práxedes Sánchez [a], Eleuterio Álvarez [a], Riccardo Peloso [a,*]

[a] Instituto de Investigaciones Químicas (IIQ), Departamento de Química Inorgánica and Centro de Innovación en Química Avanzada (ORFEO−CINQA), Consejo Superior de Investigaciones Científicas (CSIC), Universidad de Sevilla, 41092 Sevilla, Spain
[b] Dipartimento di Chimica e Chimica Industriale, Universitá di Pisa, Via G. Moruzzi 13, I-56124 Pisa, Italy
[c] Departamento de Química Inorgánica, Universidad de Sevilla, Aptdo 1203, Sevilla 41071, Spain

ARTICLE INFO

Keywords:
Phosphine ligands
X-ray structures
Group 11 metal complexes
^{31}P NMR
Sterically demanding ligands
Coordination Chemistry

ABSTRACT

Two sterically demanding tertiary phosphines, P*i*Pr$_2$Xyl and P*t*Bu$_2$Xyl, (Xyl = 2,6-dimethylphenyl), the latter reported here for the first time, have been used to synthesize a series of dinuclear complexes of the general formula [M(μ-X)PR$_2$Xyl]$_2$, (R = *i*Pr, *t*Bu; M = Cu: X = Cl, Br, I, OTf; M = Ag: X = OTf, NTf$_2$). All compounds have been characterized by multinuclear NMR spectroscopy in solution and, with the exception of AgNTf$_2$(P*t*Bu$_2$Xyl), by X-ray diffraction analyses. The doubly halido-bridged compounds [Cu(μ-X)PR$_2$Xyl]$_2$ (R = *i*Pr, *t*Bu; X = Cl, Br, I) display C_i, C_2-like, or C_1 molecular symmetry, depending on the anion and the R group, and enclose planar or disphenoidal [CuX]$_2$ cores with short, bonding Cu—Cu distances in case of X = I. On the other hand, centrosymmetric 8-membered rings with twist-chair conformations are found in the solid state structures of [M(μ-OTf)PR$_2$Xyl]$_2$ (R = *i*Pr, *t*Bu; M = Cu, Ag) and [Ag(μ-NTf$_2$)P*i*Pr$_2$Xyl]$_2$, with the anions in a κ^2-μ^2 coordination mode. Additionally, the cationic complex [Cu(PR$_2$Xyl)$_2$]$^+$ has been obtained as a triflate or BAr^F salt (BAr^{F-} = B{3,5-(CF$_3$)$_2$C$_6$H$_3$}$_4^-$), and shows C_2-like symmetry in the solid state, with PCuP angles of *ca.* 168-169° and synclinal dispositions of the Xyl groups with respect to the P•••P axis. Comparative discussion of relevant NMR data of Cu(I), Ag(I), and Au(I) adducts of the title phosphines is also provided.

1. Introduction

By virtue of the wide spectrum of finely tunable structural, steric, and electronic features that they provide to isolable coordination compounds and key-intermediates in complex chemical transformations, phosphines and related ligands of trivalent phosphorus have attracted growing interest in fundamental and applied chemistry since the second half of the past century [1–4]. Specifically, P(III) ligands with a high steric demand, combined with the appropriate metal, acted as protagonists in several landmark discoveries and processes, such as, for instance, the detection and characterization in solution of the first σ-complex of methane [5], the asymmetric catalytic hydrogenation of alkenes [6–10], the palladium catalyzed cross-coupling reactions. These outstanding findings were made possible by means of bulky mono- or polydentate ligands with P-donor atoms, often bearing biaryl, isopropyl, or *tert*-butyl substituents [11–18].

The presence of CH$_3$ groups at the *ortho* positions of P-bonded aryl radicals increases dramatically the steric requirements of the ligand, accordingly, for instance, to the Tolman cone angles of 145, 194, and 212° assigned to the triaryl phosphines PPh$_3$, P(*o*-tolyl)$_3$, and PMes$_3$ (Mes = 2,4,6-trimethylphenyl), respectively [19–21]. Corresponding values for P*i*Pr$_3$ and P*t*Bu$_3$ are 160 and 182°, respectively, which allows us to roughly estimate the cone angle of the title phosphines in the range 180-200°. In spite of the recently documented use of (2,6-dimethylphenyl)diisopropyl phosphane, P*i*Pr$_2$Xyl (Xyl = 2,6-dimethylphenyl) and its crucial role in unusual transformations and in the stabilization of elusive organometallic species involving rhodium, iridium [22], and platinum centers [23–25], we are not aware of any scientific reports on the even more sterically demanding P*t*Bu$_2$Xyl ligand. Nevertheless, the closely related P*t*Bu$_2$(*o*-tolyl) phosphine was already used in Shaw's pioneering work on cyclometallation processes dating back to the early 1970 s [26] and, more recently, by Beller and coworkers [11,12]. As far as the chemistry of group 11 metals is concerned, it is worth mentioning in this context the isolation of challenging Au(I) complexes supported by

* Corresponding author.
E-mail address: rpeloso@us.es (R. Peloso).

https://doi.org/10.1016/j.ica.2023.121623
Received 21 April 2023; Received in revised form 6 June 2023; Accepted 6 June 2023
Available online 14 June 2023

the sterically encumbered $PMes_3$ ligand [27,28].

Aiming to gain wider information on the coordination chemistry of the barely studied phosphane P*i*Pr$_2$Xyl and its bulkier congener P*t*Bu$_2$Xyl, and continuing our research on copper(I) terphenylphosphine complexes [29], we decided to undertake the synthesis of a series Cu(I) complexes with the title ligands and to explore related silver(I) chemistry. Taking advantage of the abundance of structural data gathered on the target compounds, special emphasis will be given to the discussion of conformational and geometrical aspects.

2. Experimental

All manipulations were carried out using standard Schlenk and glove-box techniques, under an atmosphere of high-purity nitrogen. Solvents were rigorously dried and degassed before use. Copper(I) halides were prepared in an aqueous medium by reduction of $CuSO_4{\cdot}5H_2O$ (1 eq) with Na_2SO_3 (2 eq) in the presence of the appropriate sodium halide (*ca.* 4 eq), isolated by filtration as colorless solids, washed with acetic acid and diethyl ether, dried *in vacuo*, and stored under nitrogen. P*i*Pr$_2$Xyl [25], CuOTf•0.5(toluene) [30], and NaBAr^F [31] were prepared as previously reported. Other chemicals were purchased from Sigma-Aldrich and used as received. ^{1}H-, ^{13}C-, and ^{31}P NMR spectra were recorded at 300, 400, and 500 MHz, using the solvent peak as the internal reference. Spectral assignments were made by routine one- and two-dimensional NMR experiments (^{1}H, ^{13}C{^{1}H}, ^{31}P{^{1}H}, COSY, HSQC and HMBC). All $^3J_{HH}$ aromatic-coupling constants in ^{1}H NMR spectra are *ca.* 7–8 Hz. For elemental analyses, a LECO TruSpec CHN elementary analyzer was utilized. A summary of crystallographic and structure refinement data for compounds **1a-d**, **2a-d**, **3d**, **3e**, **4d**, **7·BAr^F** and **7·OTf** are given in Tables S1-S13 **(**see the Supporting Information**)**.

Synthesis of P*t*Bu$_2$Xyl [32]. A 0.90 M solution of (2,6-dimethylphenyl)magnesium bromide in THF (20 mL, 18 mmol) was added dropwise to a solution of P*t*Bu$_2$Cl (3.4 mL, 18 mmol) in THF (50 mL) in the presence of CuCl (0.67 g, 6.9 mmol) at 50 °C. The reaction mixture was refluxed overnight under nitrogen and taken to dryness under reduced pressure to yield an oily residue, which was extracted in pentane (3 × 20 mL). After combining the organic phases, volatiles were removed by evaporation under reduced pressure, affording a colorless liquid substance, which was dried *in vacuo* and stored under nitrogen. Yield: 3.0 g (66%). ^{1}H NMR ($CDCl_3$, 300 MHz, 25 °C): δ 7.18–7.06 (m, 3H, aromatic CH), 2.75 (d, 3H, $^4J_{HP}$ = 3.8 Hz, CH_3 Xyl), 2.61 (s, 3H, CH_3 Xyl), 1.28 (d, 18H, $^3J_{HP}$ = 12.4 Hz, $C(CH_3)_3$) ppm. ^{31}P{^{1}H} NMR ($CDCl_3$, 121 MHz, 25 °C): δ 26.9 (s) ppm. ^{13}C{^{1}H} NMR ($CDCl_3$, 125 Hz, 25 °C): δ 148.0 (d, $^2J_{CP}$ = 38 Hz, *o*-Xyl), 142.6 (d, $^2J_{CP}$ = 6 Hz, *o*-Xyl), 134.8 (d, $^1J_{CP}$ = 41 Hz, *ipso*-Xyl), 128.7 (s, *m*-Xyl), 128.5 (d, $^4J_{CP}$ = 2 Hz, *p*-Xyl), 128.2 (d, $^3J_{CP}$ = 7 Hz, *m*-Xyl), 33.3 (d, $^1J_{CP}$ = 30 Hz, *C*$(CH_3)_3$), 31.5 (d, $^2J_{CP}$ = 17 Hz, C(*C*$H_3)_3$), 27.0 (s, CH_3 Xyl), 26.7 (s, CH_3 Xyl) ppm. Anal. Calc. for $C_{16}H_{27}P$: C, 76.76; H, 10.87. Found: C, 77.0; H, 10.5.

General synthesis of [Cu(μ-X)(PR$_2$Xyl)]$_2$ (R = *i*Pr, X = Cl, Br, I: **1a**, **1b**, **1c**; R = *t*Bu, X = Cl, Br, I: **2a**, **2b**, **2c**). Solid samples of CuX were suspended in dichloromethane solutions (*ca.* 10 mL) of PR_2Xyl in a 1:1 M ratio. The resulting mixtures were stirred at room temperature until complete disappearance of the solid phase. Elimination of the solvent by evaporation under reduced pressure afforded solid residues, which were washed with pentane and dried *in vacuo*, yielding complexes **1a-c** and **2a-c** as colorless or pale yellow solid materials. Single crystals suitable for X-ray diffraction analyses were obtained by slow cooling of *n*-heptane solutions of the compounds from *ca.* 90 °C to the room temperature.

[Cu(μ-Cl)(P*i*Pr$_2$Xyl)]$_2$, 1a. Yield: 88 mg (61%). ^{1}H NMR ($CDCl_3$, 300 MHz, 25 °C): δ 7.22 (t, 1H, *p*-Xyl), 7.03 (dd, 2H, *m*-Xyl), 2.82 (br s, 6H, CH_3 Xyl), 2.62 (sept, 2H, $^3J_{HH}$ = 6.0 Hz, C*H*$(CH_3)_2$), 1.48 (dd, 6H, $^3J_{HH}$ = 7.0 Hz, $^3J_{HP}$ = 19.7 Hz, CH(C*H*$_3$)(CH$_3$)) 0.97 (dd, 6H, $^3J_{HH}$ = 7.0 Hz, $^3J_{HP}$ = 17.1 Hz, CH(CH$_3$)(C*H*$_3$)) ppm. ^{31}P{^{1}H} NMR ($CDCl_3$, 121 MHz, 25 °C): δ 21.0 (br s) ppm. ^{13}C{^{1}H} NMR ($CDCl_3$, 101 MHz, 25 °C): δ 143.4 (br s, *o*-Xyl), 130.2 (d, $^1J_{CP}$ = 17 Hz, *ipso*-Xyl), 129.9 (s, *p*-Xyl), 128.2 (s, *m*-Xyl), 26.0 (d, $^1J_{CP}$ = 18 Hz, *C*H$(CH_3)_2$), 25.2 (br s, *C*H$_3$ Xyl), 22.2 (d, $^2J_{CP}$ = 6 Hz, CH(*C*H$_3$)(CH$_3$)), 20.4 (s, CH(CH$_3$)(*C*H$_3$)) ppm.Anal. Calc. for $C_{14}H_{23}ClCuP$: C, 52.33; H, 7.22. Found: C, 52.4; H, 7.5.

[Cu(μ-Br)(P*i*Pr$_2$Xyl)]$_2$, 1b. Yield 103 mg (63%). ^{1}H NMR ($CDCl_3$, 300 MHz, 25 °C): δ 7.16 (t, 1H, *p*-Xyl), 7.03 (d, 2H, *m*-Xyl), 2.76 (br s, 6H, CH_3 Xyl), 2.62 (sept, 2H, $^3J_{HH}$ = 7.0 Hz, C*H*$(CH_3)_2$), 1.94 (dd, 6H, $^3J_{HH}$ = 6.2 Hz, $^3J_{HP}$ = 18.5 Hz, CH(C*H*$_3$)(CH$_3$)), 0.93 (dd, 6H, $^3J_{HH}$ = 6.81 Hz, $^3J_{HP}$ = 16.0 Hz, CH(CH$_3$)(C*H*$_3$)) ppm. ^{31}P{^{1}H} NMR ($CDCl_3$, 121 MHz, 25 °C): δ 17.3 (br s) ppm. ^{13}C{^{1}H} NMR ($CDCl_3$, 101 MHz, 25 °C): δ 143.6 (br s, *o*-Xyl), 130.0 (d, $^1J_{CP}$ = 32 Hz, *ipso*-Xyl), 129.0 (s, *p*-Xyl), 128.7 (s, *m*-Xyl), 26.3 (d, $^1J_{CP}$ = 20 Hz, *C*H$(CH_3)_2$), 25.0 (br s, CH_3 Xyl), 22.2 (d, $^2J_{CP}$ = 13 Hz, CH(*C*H$_3$)(CH$_3$)), 20.2 (s, CH(CH$_3$)(*C*H$_3$)) ppm. Anal. Calc. for $C_{14}H_{23}BrCuP$: C, 45.97; H, 6.34. Found: C, 46.0; H, 6.3.

[Cu(μ-I)(P*i*Pr$_2$Xyl)]$_2$, 1c. Yield 119 mg (64%). ^{1}H NMR ($CDCl_3$, 300 MHz, 25 °C): δ 7.20 (t, 1H, *p*- Xyl), 7.07 (d, 2H, *m*-Xyl), 2.83 (br s, 6H, CH_3 Xyl), 2.77 (sept, 2H, $^3J_{HH}$ = 7.1 Hz, C*H*$(CH_3)_2$), 1.55 (dd, 6H, $^3J_{HH}$ = 7.0 Hz, $^3J_{HP}$ = 18.6 Hz, CH(C*H*$_3$)(CH$_3$)), 1.08 (dd, 6H, $^3J_{HH}$ = 7.0 Hz, $^3J_{HP}$ = 16.0 Hz, CH(CH$_3$)(C*H*$_3$)) ppm. ^{31}P{^{1}H} NMR ($CDCl_3$, 121 MHz, 25 °C): δ 19.7 (br s) ppm. ^{13}C{^{1}H} NMR ($CDCl_3$, 101 MHz, 25 °C): δ 143.7 (br s, *o*-Xyl), 130.0 (d, $^1J_{CP}$ = 25 Hz, *ipso*-Xyl), 129.1 (s, *p*-Xyl), 128.8 (s, *m*-Xyl), 26.7 (d, $^1J_{CP}$ = 18 Hz, *C*H(CH_3)), 24.7 (br, CH_3 Xyl), 21.6 (d, $^2J_{CP}$ = 13 Hz, CH(*C*H$_3$)(CH$_3$)), 20.0 (d, $^2J_{CP}$ = 5 Hz, CH(CH$_3$)(*C*H$_3$)) ppm. Anal. Calc. for $C_{14}H_{23}CuIP$: C, 40.74; H, 5.62. Found: C, 40.7; H, 5.5.

[Cu(μ-Cl)(P*t*Bu$_2$Xyl)]$_2$, 2a. Yield: 84 mg (63%). ^{1}H NMR ($CDCl_3$, 300 MHz, 25 °C): δ 7.29–7.15 (m, 3H, aromatic CH), 3.30 (d, 3H, $^4J_{HP}$ = 3.1 Hz, CH_3 Xyl), 2.65 (s, 3H, CH_3 Xyl), 1.50 (d, 18H, $^3J_{HP}$ = 16.1 Hz, C$(CH_3)_3$) ppm. ^{31}P{^{1}H} NMR ($CDCl_3$, 121 MHz, 25 °C): δ 34.8 (br s) ppm. ^{13}C{^{1}H} NMR ($CDCl_3$, 101 MHz, 25 °C): δ 145.2 (d, $^2J_{CP}$ = 20 Hz, *o*-Xyl), 142.5 (s, *o*-Xyl), 130.5 (s, *m*-Xyl), 130.4 (d, $^4J_{CP}$ = 4 Hz, *p*-Xyl), 127.8 (s, *m*-Xyl), 37.2 (d, $^1J_{CP}$ = 12 Hz, *C*$(CH_3)_3$), 31.8 (d, $^2J_{CP}$ = 10 Hz, C(*C*$H_3)_3$), 29.4 (d, $^3J_{CP}$ = 22 Hz, CH_3 Xyl), 27.3 (s, CH_3 Xyl) ppm. Anal. Calc. for $C_{16}H_{27}ClCuP$: C, 55.01; H, 7.79. Found: C, 54.7; H, 8.1.

[Cu(μ-Br)(P*t*Bu$_2$Xyl)]$_2$, 2b. Yield: 90 mg (60%). ^{1}H NMR ($CDCl_3$, 300 MHz, 25 °C): δ 7.25–7.14 (m, 3H, aromatic CH), 3.32 (d, 3H, $^4J_{HP}$ = 3.1 Hz, CH_3 Xyl), 2.66 (s, 3H, CH_3 Xyl), 1.51 (d, 18H, $^3J_{HP}$ = 15.4 Hz, C$(CH_3)_3$) ppm. ^{31}P{^{1}H} NMR ($CDCl_3$, 121 MHz, 25 °C): δ 39.3 (br s) ppm. ^{13}C{^{1}H} NMR ($CDCl_3$, 101 MHz, 25 °C): δ 145.8 (d, $^2J_{CP}$ = 21 Hz, *o*-Xyl), 142.5 (s, *o*-Xyl), 130.2 (s, *m*-Xyl), 130.1 (d, $^4J_{CP}$ = 4 Hz, *p*-Xyl), 129.0 (s, *m*-Xyl), 37.2 (d, $^1J_{CP}$ = 8 Hz, *C*$(CH_3)_3$), 31.4 (d, $^2J_{CP}$ = 10 Hz, C(*C*$H_3)_3$), 28.3 (s, CH_3 Xyl), 27.3 (s, CH_3 Xyl) ppm. Anal. Calc. for $C_{16}H_{27}BrCuP$: C, 48.80; H, 6.91. Found: C, 48.4; H, 7.3.

[Cu(μ-I)(P*t*Bu$_2$Xyl)]$_2$, 2c. Yield: 105 mg (60%). ^{1}H NMR ($CDCl_3$, 300 MHz, 25 °C): δ 7.30–7.13 (m, 3H, aromatic CH), 3.33 (d, 3H, $^4J_{HP}$ = 3.1 Hz, CH_3 Xyl), 2.65 (s, 3H, CH_3 Xyl), 1.51 (d, 18H, $^3J_{HP}$ = 15.8 Hz, C$(CH_3)_3$) ppm. ^{31}P{^{1}H} NMR ($CDCl_3$, 121 MHz, 25 °C): δ 36.9 (br s) ppm. ^{13}C{^{1}H} NMR ($CDCl_3$, 101 MHz, 25 °C): δ 146.2 (d, $^2J_{CP}$ = 23 Hz, *o*-Xyl), 142.1 (s, *o*-Xyl), 130.3 (s, $^3J_{CP}$ = 8 Hz, *m*-Xyl), 129.9 (d, $^4J_{CP}$ = 4 Hz, *p*-Xyl), 129.7 (s, *m*-Xyl), 37.3 (d, $^1J_{CP}$ = 6 Hz, *C*$(CH_3)_3$), 30.6 (d, $^2J_{CP}$ = 9 Hz, C(*C*$H_3)_3$), 27.0 (s, CH_3 Xyl), 26.8 (s, CH_3 Xyl) ppm. Anal. Calc. for $C_{16}H_{27}CuIP$: C, 43.60; H, 6.17. Found: C, 43.6; H, 5.8.

Synthesis of [Cu(μ-OTf-κ*O*:κ*O'*)(PR$_2$Xyl)]$_2$ (R = *i*Pr: **1d**; R = *t*Bu: **2d**). Neat samples of PR_2Xyl were dissolved in toluene solutions (*ca.* 5 mL) of Cu(OTf)•0.5(toluene) in a 1:1 M ratio. The resulting colorless solutions were stirred for approximately 1 h at room temperature. Upon addition of pentane (*ca.* 5 mL), colorless solid materials separated out, which were collected by filtration, washed with *n*-pentane (2 mL), and dried *in vacuo*. Crystals of **1d** and **2d** suitable for X-ray diffraction analyses were obtained by slow diffusion of *n*-pentane into benzene solutions of the compounds.

[Cu(μ-OTf-κ*O*:κ*O'*)(P*i*Pr$_2$Xyl)]$_2$, 1d. Yield: 92 mg (55%). ^{1}H NMR ($CDCl_3$, 300 MHz, 25 °C): δ 6.84 (t, 1H, *p*-Xyl), 6.70 (d, 2H, *m*-Xyl), 2.46 (br s, 6H, CH_3 Xyl), 1.98 (sept, 2H, $^3J_{HH}$ = 7.1 Hz, C*H*$(CH_3)_2$), 1.15 (dd, 6H, $^3J_{HH}$ = 7.1 Hz, $^3J_{HP}$ = 18.4 Hz, CH(C*H*$_3$)(CH$_3$)), 0.69 (dd, 6H, $^3J_{HH}$ = 7.1 Hz, $^3J_{HP}$ = 16.0 Hz, CH(CH$_3$)(C*H*$_3$)) ppm. ^{31}P{^{1}H} NMR (121 MHz, C_6D_6, 25 °C): δ 24.3 (br s) ppm. Anal. Calc. for $C_{15}H_{23}CuF_3O_3PS$: C,

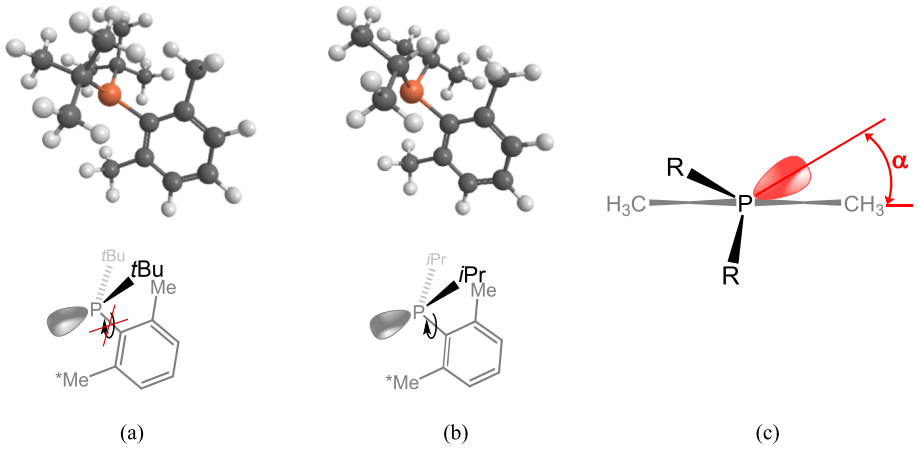

Fig. 1. 3D-representations of the conformers observed for the phosphine ligands P*t*Bu$_2$Xyl (a) and P*i*Pr$_2$Xyl (b), and definition of the dihedral angle, α (c).

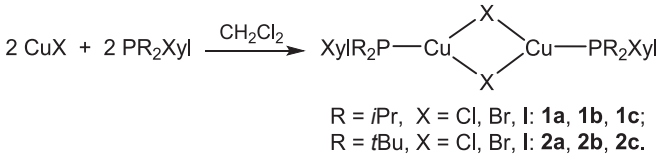

Scheme 1. Synthesis of the dinuclear copper(I) complexes **1a-c** and **2a-c**.

41.42; H, 5.33. Found: C, 41.1; H, 5.0.

[Cu(μ-OTf-κ*O*:κ*O'*)(P*t*Bu$_2$Xyl)] $_2$, 2d. Yield: 87 mg (49%). ^{1}H NMR ($CDCl_3$, 300 MHz, 25 °C): δ 7.30–7.20 (m, 6H, aromatic CH), 3.16 (d, 3H, $^4J_{HP}$ = 3.8 Hz, CH_3 Xyl), 2.65 (s, 3H, CH_3 Xyl), 1.44 (d, 18H, $^3J_{HP}$ = 16.3 Hz, $C(CH_3)_3$) ppm. $^{31}P\{^1H\}$ NMR (121 MHz, CD_2Cl_2, 25 °C): δ 44.7 (br s) ppm. Anal. Calc. for $C_{17}H_{27}CuF_3O_3PS$: C, 44.10; H, 5.88. Found: C, 44.1; H, 5.5.

Synthesis of [Ag(μ-X)(PR$_2$Xyl)] $_2$ (R = *i*Pr, X = OTf, NTf_2: **3d**, **3e**; R = *t*Bu, X = OTf, NTf_2: **4d**, **4e**). Equimolar neat samples of AgX and PR_2Xyl were dissolved at 0 °C in *ca.* 5 mL of THF (X = OTf) or toluene (X = NTf_2). After 30 min stirring, volatiles were removed by evaporation under reduced pressure. The resulting oily materials were washed with 2 mL of diethyl ether (X = OTf) or pentane (X = NTf_2) to obtain colorless solids, which were collected by filtration and dried *in vacuo*. Adventitious impurities due to decomposition of the silver precursors, which frequently darken the solid samples of complexes **3** and **4**, were removed by dissolving the crude solid materials in CH_2Cl_2, followed by filtration through Celite® and evaporation of the solvent. Crystals of **3d**, **4d**, and **3e** suitable for X-ray diffraction analyses were obtained by slow diffusion of *n*-heptane into dichloromethane solutions of the compounds.

[Ag(μ-OTf-κ*O*:κ*O'*)(P*i*Pr$_2$Xyl)] $_2$, 3d. Yield: 107 mg (50%). ^{1}H NMR ($CDCl_3$, 300 MHz, 25 °C): δ 6.95 (t, 1H, *p*-Xyl), 6.80 (d, 2H, *m*-Xyl), 2.47 (br s, 6H, CH_3 Xyl), 2.11 (sept, 2H, $^3J_{HH}$ = 7.2 Hz, C*H*$(CH_3)_2$), 1.19 (dd, 6H, $^3J_{HH}$ = 7.2 Hz, $^3J_{HP}$ = 21.3 Hz, CH$(CH_3)(CH_3)$), 0.74 (dd, 6H, $^3J_{HH}$ = 7.2 Hz, $^3J_{HP}$ = 18.0 Hz, CH$(CH_3)(CH_3)$) ppm. $^{31}P\{^1H\}$ NMR (121 MHz,

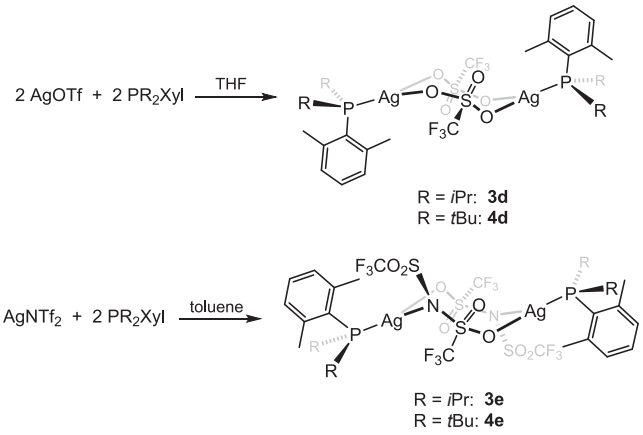

Scheme 3. Synthesis of the silver(I) complexes **3-4d** (top) and **3-4e** (bottom).

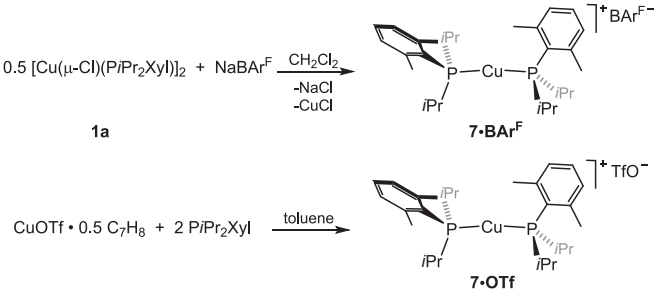

Scheme 4. Synthesis of the cationic copper(I) complexes **7·BAr^F** (top) and **7·OTf** (bottom), depicted according to the conformations found in the solid state.

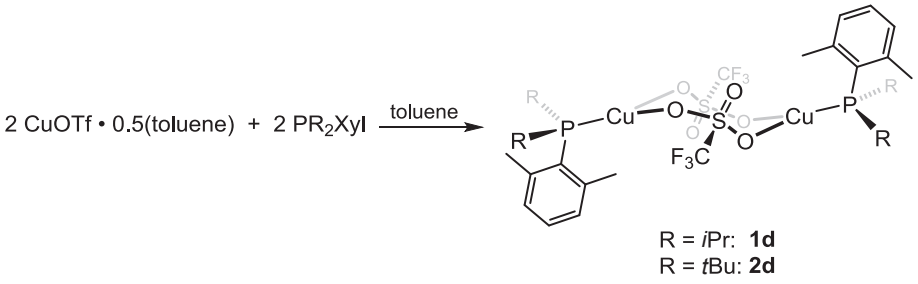

Scheme 2. Synthesis of the dinuclear copper(I) complexes **1d** and **2d**.

Table 1
Relevant $^{31}P\{^{1}H\}$ NMR data for complexes **1–6** ($CDCl_3$, 25 °C, unless otherwise stated).

	M ($^{+}$)	anion ($^{-}$)	δ ^{31}P (ppm)	$\bar{\delta}$ [a] *(ppm)*	multiplicity	J_{Rg}^{107} (Hz)	$^{1}J_{Rg}^{109}$ (Hz)
P*i*Pr$_2$Xyl			7.2		s		
1a	Cu	Cl	21.0	*21*	s (br)		
1b	Cu	Br	17.3		s (br)		
1c	Cu	I	19.7		s (br)		
1d (C_6D_6)	Cu	OTf	24.3		s (br)		
3d	Ag	OTf	32.6	*34*	d	705	814
3e	Ag	NTf_2	36.2		d	681	786
5a	Au	Cl	52.1	*52*	s		
P*t*Bu$_2$Xyl			26.9		s		
2a	Cu	Cl	34.8	*39*	s (br)		
2b	Cu	Br	39.3		s (br)		
2c	Cu	I	36.9		s (br)		
2d (CD_2Cl_2)	Cu	OTf	44.7		s (br)		
4d	Ag	OTf	52.7	*53*	d	705	823
4e	Ag	NTf_2	52.4		d	685	791
6a	Au	Cl	69.4	*69*	s		

[a] *average.*

Table 2
Selected structural data for complexes **1a-c** and **2a-c** in the solid state.

[CuX(PR$_2$Xyl)] $_2$	R	X	Cu-Cu (Å)	Cu-P (Å)	Core planarity (°)[a]	CuXCu (°)	α[b] (°)	Point Group
1a	*i*Pr	Cl	3.02	2.19	yes (0)	82.0	12	C_i
2a	*t*Bu	Cl	2.91	2.21	no (34)	76.6	16[c]	C_1
1b	*i*Pr	Br	2.90	2.21	no (49)	73.3	14[c]	C_2[d] (C_1)
2b	*t*Bu	Br	3.07	2.23	yes	77.4	22	C_i
1c	*i*Pr	I	2.85	2.24[c]	no (48)	66.7	17[c]	C_2[d] (C_1)
2c	*t*Bu	I	2.78	2.27	yes	64.6	29	C_i

[a] dihedral angle between the coordination planes of the two Cu atoms;
[b] torsion angle $CC_{Xyl}PCu$, as represented in Fig. 1c;
[c] average;
[d] approximate symmetry, *i.e.* reached by slight modifications of *x*,*y*, *z* coordinates (point group found in the X-ray structure).

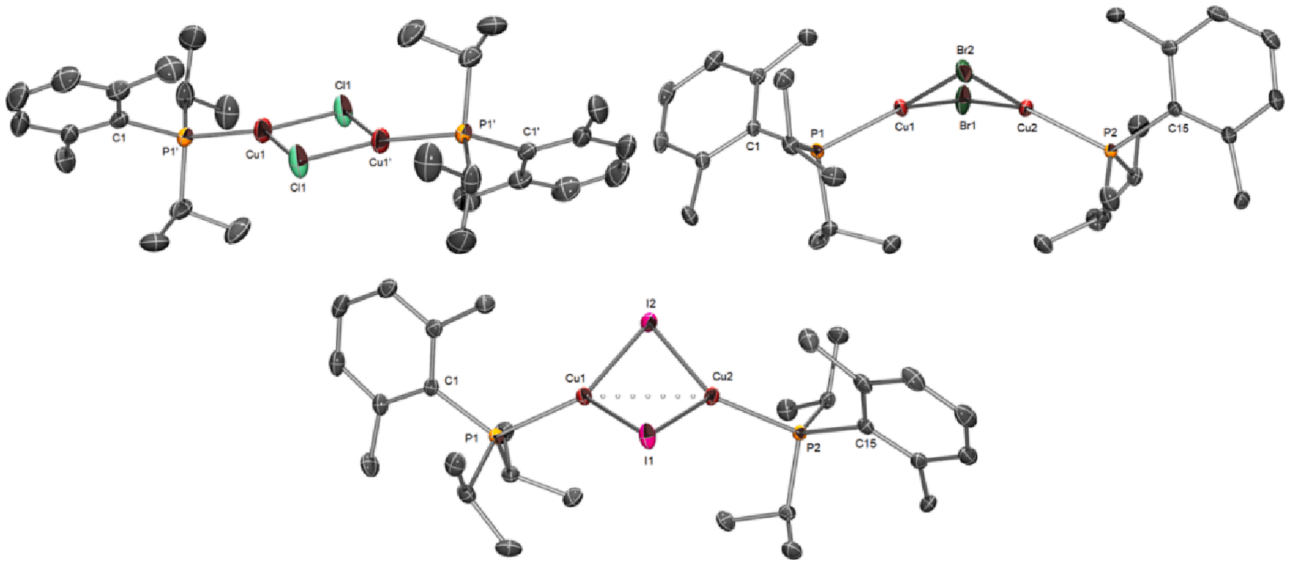

Fig. 2. ORTEP views of the molecular structures of complexes **1a** (top left), **1b** (top right), and **1c** in the solid state (bottom).

$CDCl_3$, 25 °C): δ 32.6 (d, $^{1}J_{Rg}^{107}$ = 705 Hz, $^{1}J_{Rg}^{109}$ = 814 Hz) ppm. $^{13}C\{^{1}H\}$ NMR ($CDCl_3$, 125 Hz, 25 °C): δ 142.9 (br s, *o*-Xyl), 131.1 (s, *p*-Xyl), 130.6 (d, $^{3}J_{CP}$ = 6 Hz, *m*-Xyl), 126.1 (d, $^{1}J_{CP}$ = 20 Hz, *ipso*-Xyl), 26.0 (d, $^{1}J_{CP}$ = 19 Hz, *C*H(CH$_3$)$_2$), 24.9 (br s, CH$_3$ Xyl), 23.6 (d, $^{2}J_{CP}$ = 15 Hz, CH(*C*H$_3$)(CH$_3$)), 20.9 (d, $^{2}J_{CP}$ = 7 Hz, CH(CH$_3$)(*C*H$_3$)) ppm. Anal. Calc. for $C_{15}H_{23}AgF_3O_3PS$: C, 37.59; H, 4.84. Found: C, 37.4; H, 5.1.

[Ag(μ-NTf$_2$-κ*N*:κ*O*)(P*i*Pr$_2$Xyl)] $_2$, 3e. Yield: 122 mg (44%). ^{1}H NMR ($CDCl_3$, 300 MHz, 25 °C): δ 6.94 (t, 1H, *p*-Xyl), 6.76 (d, 2H, *m*-Xyl), 2.29 (br s, 6H, CH$_3$ Xyl), 1.96 (sept, 2H, $^{3}J_{HH}$ = 6.5 Hz, C*H*(CH$_3$)$_2$), 0.99 (dd, 6H, $^{3}J_{HH}$ = 6.5 Hz, $^{3}J_{HP}$ = 21.8 Hz, CH(*C*H$_3$)(CH$_3$)), 0.52 (dd, 6H, $^{3}J_{HH}$ = 6.5 Hz, $^{3}J_{HP}$ = 18.1 Hz, CH(CH$_3$)(*C*H$_3$)) ppm. $^{31}P\{^{1}H\}$ NMR ($CDCl_3$, 162 MHz, 25 °C): δ 37.2 (d, $^{1}J_{Rg}^{107}$ = 681 Hz, $^{1}J_{Rg}^{109}$ = 786 Hz) ppm. $^{13}C\{^{1}H\}$ NMR ($CDCl_3$, 100 MHz, 25 °C): δ 142.5 (br s, *o*-Xyl), 131.1 (s, *p*-Xyl), 130.8 (br s, *m*-Xyl), 125.0 (d, $^{1}J_{CP}$ = 20 Hz, *ipso*-Xyl), 25.9 (d, $^{1}J_{CP}$ = 19 Hz, *C*H(CH$_3$)$_2$), 24.8 (br s, CH$_3$ Xyl), 23.9 (d, $^{2}J_{CP}$ = 15 Hz, CH(*C*H$_3$)(CH$_3$)), 21.2 (d, $^{2}J_{CP}$ = 7 Hz, CH(CH$_3$)(*C*H$_3$)) ppm. Anal. Calc. for

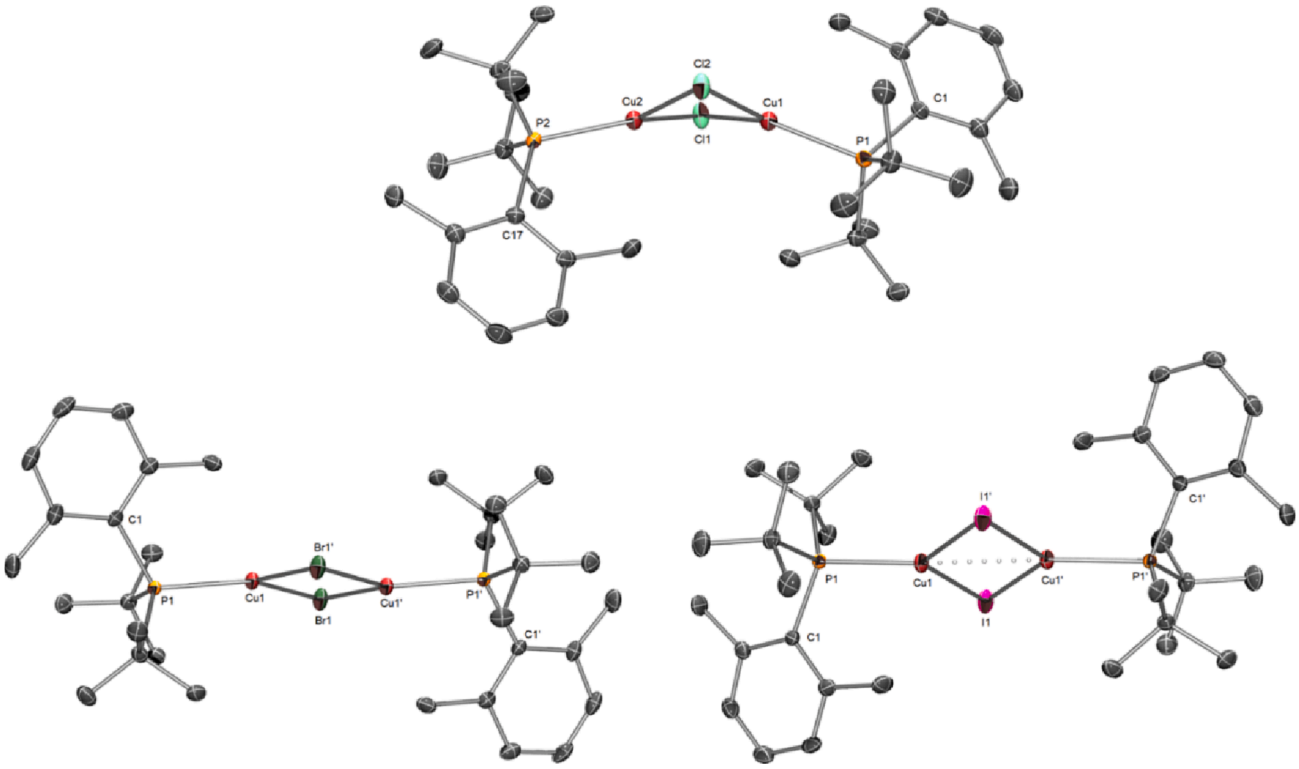

Fig. 3. ORTEP views of the molecular structures of complexes **2a** (top left), **2b** (top right), and **2c** (bottom) in the solid state.

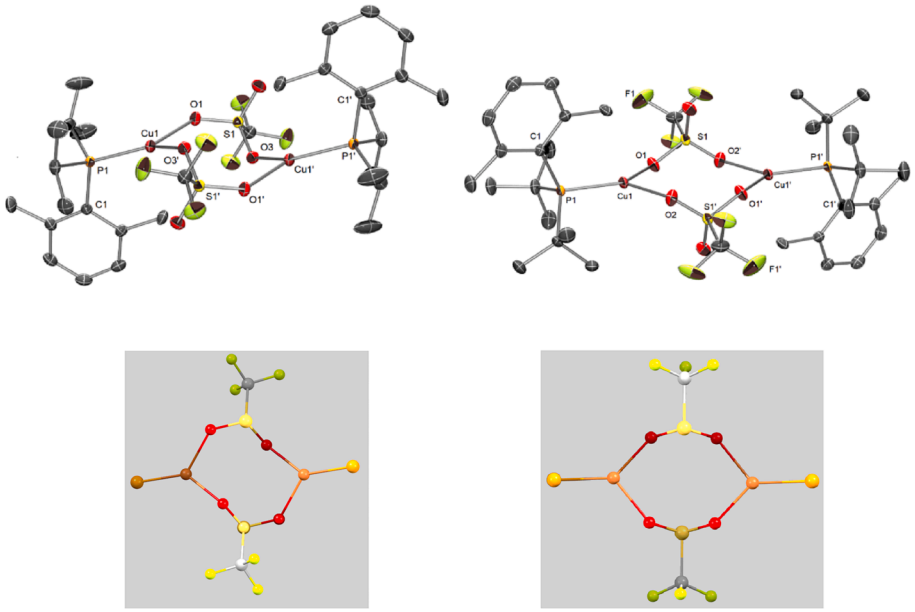

Fig. 4. ORTEP diagrams of the molecular structures of complexes **1d** (left) and **2d** (right) in the solid state (top), and simplified views perpendicular to the mid-planes of the 8-membered rings (bottom). Shaded colors in the bottom images represent objects situated below the mid-plane.

$C_{16}H_{23}AgF_6NO_4PS_2$: C, 31.49; H, 3.80. Found: C, 31.8; H, 4.0.

[Ag(μ-OTf-κ*O*:κ*O'*)(P*t*Bu$_2$Xyl)]$_2$, 4d. Yield: 122 mg (60%). ^{1}H NMR ($CDCl_3$, 300 MHz, 25 °C): δ 7.33–7.13 (m, 3H, aromatic CH), 3.09 (s, 3H, CH_3 Xyl), 2.65 (s, 3H, CH_3 Xyl), 1.47 (d, 18H, $^3J_{HP}$ = 16.3 Hz, C$(CH_3)_3$) ppm. ^{31}P{^{1}H} NMR ($CDCl_3$, 121 MHz, 25 °C): δ 52.7 (d, $^1J_{Ag}^{107}$ = 705 Hz, $^1J_{Ag}^{109}$ = 823 Hz) ppm. ^{13}C{^{1}H} NMR ($CDCl_3$, 126 MHz, 25 °C): δ 143.8 (d, $^2J_{CP}$ = 15 Hz, *o*-Xyl), 142.8 (d, $^2J_{CP}$ = 9 Hz, *o*-Xyl), 132.0 (d, $^1J_{CP}$ = 11 Hz, *ipso*-C Xyl), 130.5 (s, *m*-Xyl), 129.2 (s, *p*-Xyl), 125.9 (s, *m*-Xyl), 119.6 (q, $^1J_{CF}$ = 322 Hz, CF_3), 37.6 (d, $^1J_{CP}$ = 10 Hz, *C*$(CH_3)_3$), 29.2 (s, C$(CH_3)_3$), 27.9 (d, $^2J_{CP}$ = 27 Hz, CH_3 Xyl), 27.2 (s, CH_3 Xyl) ppm. Anal. Calc. for $C_{17}H_{27}AgF_3O_3PS$: C, 40.25; H, 5.36. Found: C, 40.0; H, 5.2.

[AgNTf$_2$(P*t*Bu$_2$Xyl)]$_2$, 4e. Yield: 124 mg (48%). ^{1}H NMR ($CDCl_3$, 300 MHz, 25 °C): δ 7.34–7.14 (m, 3H, aromatic CH), 3.05 (d, 3H, $^4J_{HP}$ = 4.1 Hz, CH_3 Xyl), 2.65 (s, 3H, CH_3 Xyl), 1.46 (d, 18H, $^3J_{HP}$ = 17.0 Hz, C$(CH_3)_3$) ppm. ^{31}P{^{1}H} NMR ($CDCl_3$, 121 MHz, 25 °C): δ 52.4 (d, $^1J_{Ag}^{107}$ = 685 Hz, $^1J_{Ag}^{109}$ = 791 Hz) ppm. Anal. Calc. for $C_{18}H_{27}AgF_6NO_4PS_2$: C, 33.87; H, 4.26. Found: C, 33.7; H, 4.3.

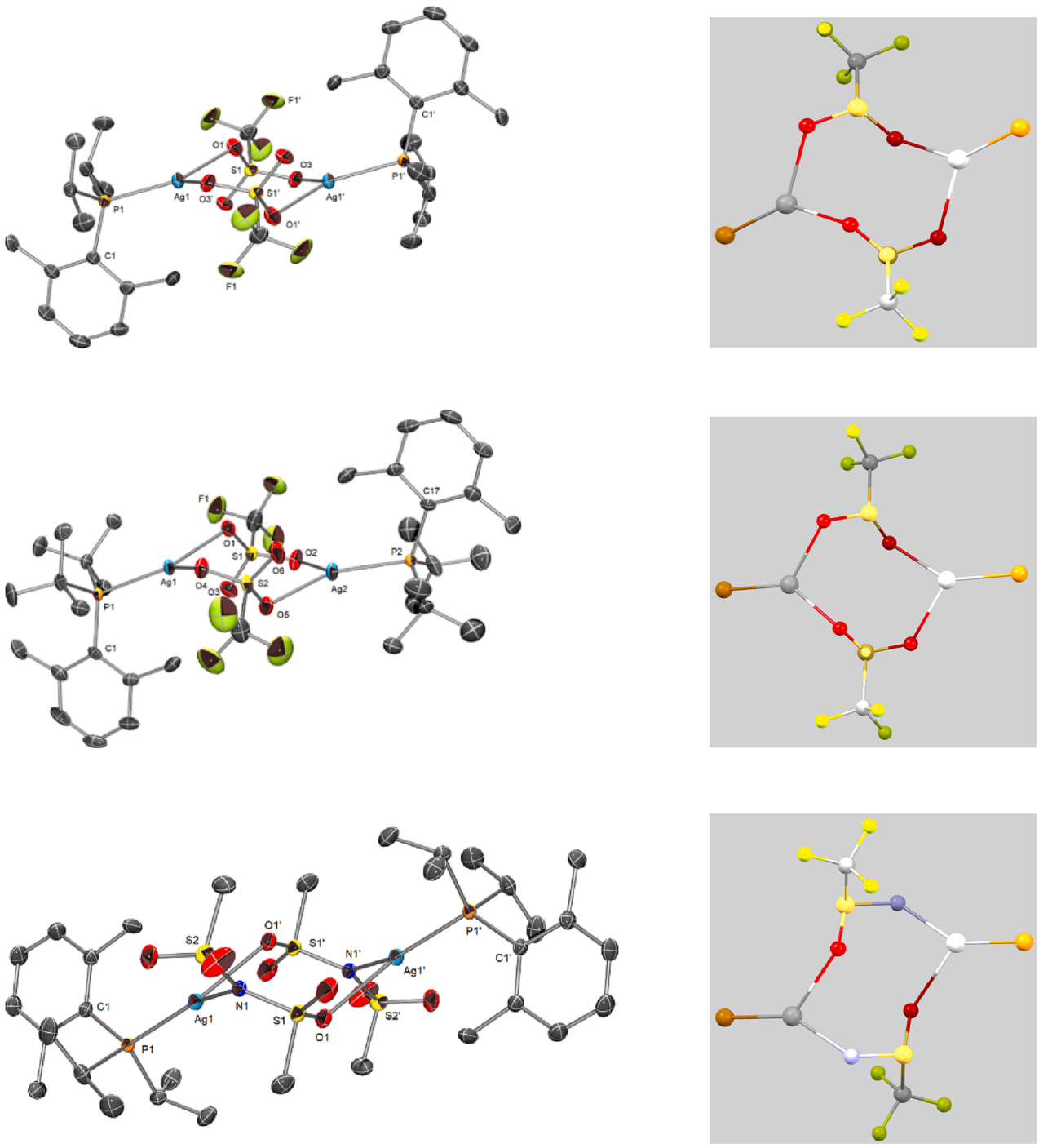

Fig. 5. ORTEP diagrams of the molecular structures of complexes **3d** (top), **4d** (middle), and **3e** (bottom) in the solid state (left), and simplified views perpendicular to the mid-planes of the 8-membered rings (right). Fluorine atoms in the ORTEP representation of **3e** have been omitted for clarity. Shaded colors in the images on the right represent objects situated below the mid-plane.

Synthesis of AuCl(PR$_2$Xyl) (R = *i*Pr: **5a**; R = *t*Bu: **6a**). Neat samples of PR$_2$Xyl and AuCl(THT) in a 1:1 M ratio were dissolved in *ca.* 5 mL dichloromethane and allowed to react overnight at room temperature. The resulting solutions were taken to dryness under reduced pressure, affording colorless solid materials, which were washed with *n*-pentane (2 mL), and dried *in vacuo*.

AuCl(P*i*Pr$_2$Xyl), 5a. Yield: 160 mg (52%). ^{1}H NMR (CDCl$_3$, 300 MHz, 25 °C): δ 7.28 (t, 1H, *p*-Xyl), 7.13 (d, 2H, *m*-Xyl), 2.90 (br s, 6H, CH$_3$ Xyl), 2.80 (sept, 2H, $^3J_{HH}$ = 7.0 Hz, C*H*(CH$_3$)$_2$), 1.48 (dd, 6H, $^3J_{HH}$ = 7.0 Hz, $^3J_{HP}$ = 19.8 Hz, CH(C*H*$_3$)(CH$_3$)), 1.01 (dd, 6H, $^3J_{HH}$ = 7.0 Hz, $^3J_{HP}$ = 18.6 Hz, CH(CH$_3$)(C*H*$_3$)) ppm. ^{31}P{^{1}H} NMR (CDCl$_3$, 121 MHz, 25 °C): δ 52.1 (s) ppm. ^{13}C{^{1}H} NMR (CDCl$_3$, 101 MHz, 25 °C): δ 142.9 (br s, *o*-C Xyl), 131.2 (d, $^1J_{CP}$ = 8 Hz, *ipso*- Xyl), 125.4 (s, *p*-Xyl), 124.9 (s, *m*-Xyl), 28.5 (d, $^1J_{CP}$ = 32 Hz, *C*H(CH$_3$)$_2$), 26.5 (br s, CH$_3$ Xyl), 23.3 (d, $^2J_{CP}$ = 7 Hz, CH(*C*H$_3$)(CH$_3$), 20.1 (d, $^2J_{CP}$ = 3 Hz, CH(CH$_3$)(*C*H$_3$)) ppm. Anal. Calc. for C$_{14}$H$_{23}$AuClP: C, 36.98; H, 5.10. Found: C, 36.8; H, 5.0.

AuCl(P*t*Bu$_2$Xyl), 6a. Yield: 190 mg (65%). ^{1}H NMR (CDCl$_3$, 300 MHz, 25 °C): δ 7.23–7.14 (m, 3H, aromatic CH), 3.51 (s, 3H, CH$_3$ Xyl), 2.67 (s, 3H, CH$_3$ Xyl), 1.57 (d, 18H, $^3J_{HP}$ = 16.5 Hz, C(CH$_3$)$_3$) ppm. ^{31}P{^{1}H} NMR (CDCl$_3$, 121 MHz, 25 °C): δ 69.4 (s) ppm. ^{13}C{^{1}H} NMR (CDCl$_3$, 125.76 Hz, 25 °C): δ 145.7 (d, $^2J_{CP}$ = 20 Xyl, *o*-Xyl), 142.5 (d, $^2J_{CP}$ = 3 Hz, *o*-Xyl), 132.0 (d, $^1J_{CP}$ = 10 Hz, *ipso*-Xyl), 130.9 (d, $^3J_{CP}$ = 3

Table 3
Selected structural data for complexes **1-4d** and **3e** in the solid state.

$[MX(PR_2Xyl)]_2$	M	R	X	M—O(N) (Å)	OMO(N) (°)	M—P (Å)	α[a] (°)	β[b] (°)	Point Group
1d[c]	Cu	*i*Pr	OTf	2.07[d]	95.0[d]	2.18[d]	12[d]	0	C_i
2d	Cu	*t*Bu	OTf	2.07[d]	99.1	2.18	13	0	C_i
3d	Ag	*i*Pr	OTf	2.36[d]	90.1	2.38	4	0	C_i
4d	Ag	*t*Bu	OTf	2.36[d]	90.0	2.41[d]	11[d]	11	C_i[e] (C_1)
3e	Ag	*i*Pr	NTf_2	2.60 (2.26)	80.9	2.38	2	0	C_i

[a] torsion angle $CC_{Xyl}PM$, as represented in Fig. 1c;
[b] dihedral angle between the mid-coordination planes of the two M atoms;
[c] two independent half-molecules in the asymmetric unit;
[d] average;
[e] approximate symmetry, *i.e.* reached by slight modifications of *x*,*y*, *z* coordinates (point group found in the X-ray structure).

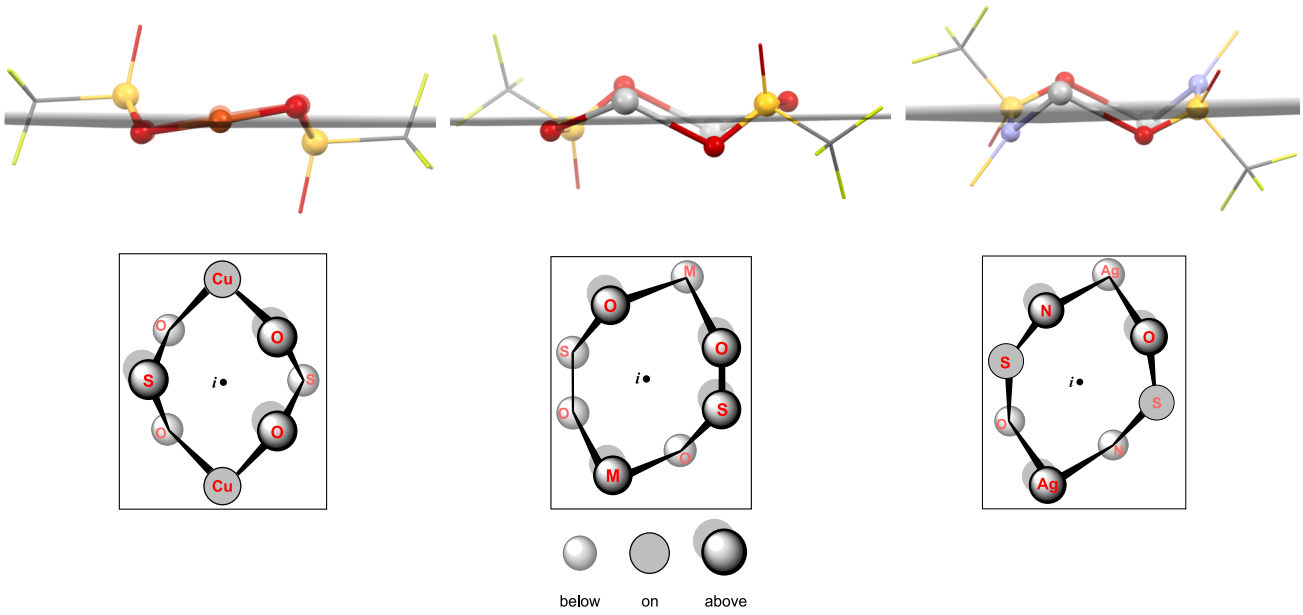

Fig. 6. Views of the centrosymmetric 8-membered rings in **2d** (left), **3d** (middle), and **3e** (right) along the corresponding mid-planes (top line), and schematic views perpendicular to them (bottom line). Complexes **1d** and **4d** adopt analogous conformations to that found for **3d**.

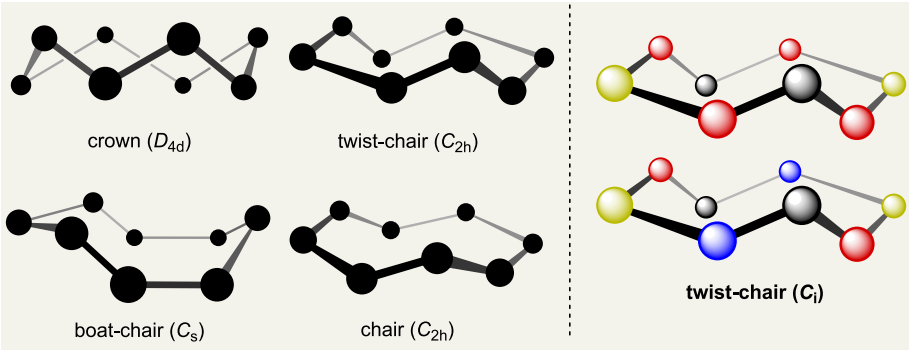

Fig. 7. Four canonical conformations of 8-membered rings (left) and idealized representation of the twist-chair conformations (C_i symmetry) adopted in the solid state by the $[M(OTf)]_2$ and $[Ag(NTf_2)]_2$ cores in **1-4d** and **3e**, respectively (right).

Hz, *m*-Xyl), 130.7 (d, $^4J_{CP}$ = 3 Hz, *p*-Xyl), 128.2 (d, $^3J_{CP}$ = 7 Hz, *m*-Xyl), 41.0 (d, $^1J_{CP}$ = 21 Hz, $C(CH_3)_3$), 32.5 (d, $^2J_{CP}$ = 7 Hz, $C(CH_3)_3$), 30.8 (d, $^2J_{CP}$ = 15 Hz, CH_3 Xyl), 28.1 (s, CH_3 Xyl) ppm. Anal. Calc. for $C_{16}H_{27}AuClP$: C, 39.81; H, 5.64. Found: C, 39.7; H, 5.8.

Synthesis of [Cu(P*i*Pr$_2$Xyl)$_2$] BAr^F, 7•BAr^F. Solid samples of complex **1a** (40 mg, 0.062 mmol) and $NaBAr^F$ (55 mg, 0.062 mmol) were dissolved in *ca.* 5 mL of dichloromethane and allowed to stir overnight at room temperature. Solid materials were filtered off and the colorless solution was concentrated to *ca.* 2 mL under reduced pressure. Upon addition of *n*-pentane a colorless solid material separated out, which was collected by filtration and dried *in vacuo*. Yield: 52 mg, 61%. Crystals suitable for X-ray diffraction were obtained by slow diffusion of *n*-pentane into saturated solutions the compound in dichloromethane. ^1H NMR (300 MHz, CD_2Cl_2, 25 °C): δ 7.78 (s, 8H, *o*-BAr^F), 7.60 (s, 4H, *p*-

Table 4
Selected structural data for complexes **7·BAr^F** and **7·OTf** in the solid state.

[Cu(P*i*Pr$_2$Xyl)$_2$] X	X	Cu-*P1* (Å)	Cu-*P2* (Å)	P1CuP2 (°)	α[a] (°)	Point Group
7·BAr^F	BAr^{F-}	2.237 (2)	2.238 (2)	169.40 (7)	12.5	C_2[b](C_1)
7·OTf	OTf$^-$	2.237 (1)	2.233 (1)	168.41 (5)	2.5 15.8	C_2[b](C_1)

[a] torsion angle CC$_{Xyl}$PCu, as represented in Fig. 1c;
[b] approximate symmetry, *i.e.* reached by slight modifications of *x*,*y*, *z* coordinates (point group found in the X-ray structure).

BAr^F), 7.38 (t, 2H, *p*-Xyl), 7.24 (d, 4H, *m*-Xyl), 2.92 (m, 4H, C*H*(CH$_3$)$_2$), 2.81 (s, 12H, CH$_3$ Xyl), 1.56 (dd, 12H, $^3J_{HH}$ = 6.4 Hz, $^3J_{HP}$ = 19.5 Hz, CH(*CH*$_3$)(CH$_3$)), 1.08 (dd, 12H, $^3J_{HH}$ = 6.4 Hz, $^3J_{HP}$ = 16.1 Hz, CH(CH$_3$)(*CH*$_3$)) ppm. ^{31}P{^{1}H} NMR (121 MHz, CD_2Cl_2, 25 °C): δ 21.6 (br s) ppm. Anal. Calc. for $C_{60}H_{58}BCuF_{24}P_2$: C, 52.55; H, 4.26. Found: C, 52.2; H, 3.9.

Synthesis of [Cu(P*i*Pr$_2$Xyl)$_2$] OTf, 7•OTf. CuOTf•0.5(toluene) (75 mg, 0.29 mmol) and P*i*Pr$_2$Xyl (130 mg, 0.58 mmol) were dissolved in *ca.* 10 mL of toluene and allowed to react approximately 30 min at room temperature. Upon addition of *n*-pentane, a colorless solid material separated out, which was collected by filtration and dried *in vacuo*. Yield: 130 mg, 690%. Crystals suitable for X-ray diffraction were obtained by slow diffusion of *n*-pentane into saturated solutions the compound in dichloromethane. ^{1}H NMR (300 MHz, C_6D_6, 25 °C): δ 6.84 t, 2H, *p*-Xyl), 6.70 (d, 4H, *m*-Xyl), 2.46 (br s, 12H, CH$_3$ Xyl), 1.98 (m, 4H, C*H*(CH$_3$)$_2$), 1.15 (dd, 12H, $^3J_{HH}$ = 6.4 Hz, $^3J_{HP}$ = 19.1 Hz, CH(CH$_3$)(*CH*$_3$)), 0.69 (dd, 12H, $^3J_{HH}$ = 6.4 Hz, $^3J_{HP}$ = 16.2 Hz, CH(CH$_3$)(*CH*$_3$)) ppm. ^{31}P{^{1}H} NMR (121 MHz, C_6D_6, 25 °C): δ 24.3 (br s) ppm. Anal. Calc. for $C_{29}H_{46}CuF_3O_3P_2S$: C, 54.32; H, 7.23. Found: C, 54.2; H, 7.0.

3. Results and discussion

The synthesis of P*t*Bu$_2$Xyl from PCl*t*Bu$_2$ and XylMgBr (Xyl = 2,6-dimethylphenyl) was performed following a slightly modified version of a procedure patented in 2003 for P*t*Bu$_2$(*o*-tolyl) [32], which requires catalytic amounts of CuCl. Di(*tert*-butyl)(2,6-dimethylphenyl)phosphane was isolated as a colorless, air-sensitive, oily substance, which can be manipulated in the air for up to some hours without appreciable oxidation. Multinuclear NMR characterization of the new ligand in $CDCl_3$ was carried out and, next, relevant date will be commented. The ^{31}P nucleus resonates as a sharp singlet at 26.9 ppm in the ^{31}P{^{1}H} NMR, whereas the ^{1}H NMR spectrum consists of three groups of signals: *i*) a multiplet at *ca.* 7 ppm for the aromatic protons; *ii*) a doublet with $^4J_{HP}$ = 3.8 Hz and a singlet at *ca.* 2.6–2.7 ppm for the benzylic protons; ii) a doublet at 1.28 ppm with $^3J_{HP}$ = 12.4 Hz for the *t*Bu groups. Interestingly, the two methyl group of the xylyl fragment give rise to two well-defined and separated resonances, which demonstrates that the two bulky P-bonded *t*Bu groups hamper the rotation of the aromatic ring around the P—C$_{Xyl}$ bond on the NMR time scale (Fig. 1a). Conversely, the benzylic protons of P*i*Pr$_2$Xyl give rise, under similar conditions, to a broad resonance, thus indicating slow rotation of the aromatic ring (Fig. 1b), and convert into a sharp singlet upon heating above 60 °C.

Fig. 1c provides a representation of the dihedral angle, α, defined by the xylyl plane and the plane containing the P—C$_{Xyl}$ bond and the axis of the P lone pair. This angular parameter quantifies the deviation of the P lone pair from the xylyl plane. Analogous parameters have recently been considered to discuss the conformation adopted by free or coordinated terphenyl phoshines, PR$_2$Ar', and found to be close to 0° in the presence of sterically demanding R groups at the P atom, such as *i*Pr or cyclohexyl [29,33]. By analogy and in agreement with the NMR data discussed above, α is expected to be approximately 0° for the ground states of P*i*Pr$_2$Xyl and P*t*Bu$_2$Xyl, which would consequently have C_s-like symmetry.

Compounds of the general formula CuX(PR$_2$Xyl), **1a-c** and **2a-c** (**1**: R = *i*Pr; **2**: R = *t*Bu; **a**: X = Cl; **b**: X = Br; **c**: X = I), were prepared by treating solid samples of the corresponding copper(I) halide with equimolar amounts of P*i*Pr$_2$Xyl or P*t*Bu$_2$Xyl, respectively, in dichloromethane. Quantitative conversions were reached in all cases over 24 h stirring at room temperature, as inferred by the slow consumption and complete disappearance of the solid phase, *i.e.* CuX, from the reaction mixture with concomitant formation of the highly soluble Cu(I) complexes (Scheme 1). These were isolated as air-stable colorless or pale yellow solid substances, highly soluble in chlorinated and aromatic organic solvents and tetrahydrofuran, and poorly soluble in diethylether and saturated hydrocarbons at room temperature.

^{31}P{^{1}H} NMR spectra of complexes **1a-c** and **2a-c** in $CDCl_3$ consist of broad singlets in the ranges 17–21 and 34–39 ppm, respectively, with low-field shifts of *ca.* 10–15 ppm with respect to the free phosphine ligands. As far as chemical shifts and multiplicities of the resonances are concerned, ^{1}H and ^{13}C{^{1}H} NMR data for **1a-c** and **2a-c** are very similar to those of P*i*Pr$_2$Xyl and P*t*Bu$_2$Xyl, respectively; hence they do not

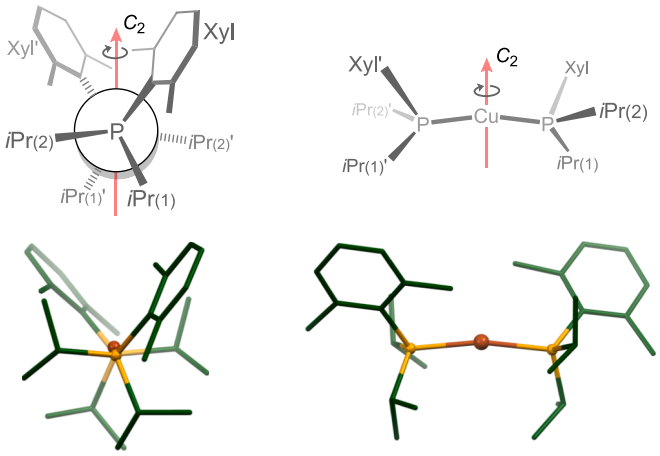

Fig. 9. Idealized C_2 symmetry for complexes **7**$^+$ (top) viewed along the P••••P axis (left) and perpendicular to it (right), and comparison with the corresponding views of the X-ray structures of **7**$^+$ in **7·OTf** (bottom).

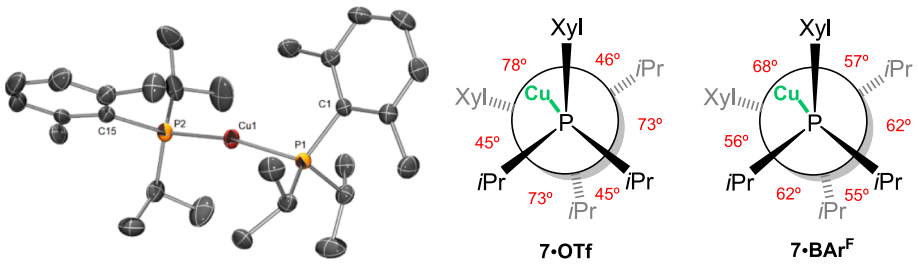

Fig. 8. ORTEP view of the cationic complex **7**$^+$ in **7·OTf** (left) and Newman-like projections sighting down the P•••P axis of the conformers observed in the X-ray structures of **7·OTf** and **7·BAr^F**, with the corresponding CP1•••P2C dihedral angles (right).

deserve any further comments.

In order to gain deeper insight into the coordination chemistry of group 11 metals in combination with P*i*Pr$_2$Xyl and P*t*Bu$_2$Xyl, we decided to explore the reactions of both phosphanes with other commonly used starting materials in Cu(I) and Ag(I) coordination chemistry, namely CuOTf•0.5(toluene), AgOTf and AgNTf$_2$ (Schemes 2 and 3). These were performed in toluene or THF at room temperature and produced, rapidly and selectively, the dinuclear triflato- and triflimidato complexes [M(μ-OTf-κ*O*:κ*O'*)(PR$_2$Xyl)]$_2$, **1-4d** (M = Cu: R = *i*Pr, *t*Bu: **1d**, **2d**; M = Ag: R = *i*Pr, *t*Bu: **3d**, **4d**), and [Ag(μ-NTf$_2$-κ*N*:κ*O*)(PR$_2$Xyl)]$_2$, **3-4e** (R = *i*Pr, *t*Bu: **3e**, **4e**), as air-sensitive colorless solid substances with high solubility in ethers, aromatic and chlorinated organic solvents.Scheme 4.

The ^{31}P{^{1}H} NMR spectra of complexes **1d** and **2d** consist of broad singlets centered at 24.3 and 44.7 ppm, respectively, slightly down-field shifted compared to the related halide adducts **1a-c** and **2a-c**, whereas their ^{1}H NMR spectra substantially parallel those of the free phosphines. The only relevant observation in this regard, which also apply to **1a-c** and **2a-c**, relates to the down-field shift of the two resonances generated by the benzylic protons of P*t*Bu$_2$Xyl upon coordination. As a matter of fact, one of them, which appears at 2.75 ppm in the free ligand, is displaced to higher frequencies (up to 3.5 ppm) in the corresponding complexes, whereas the other one remains almost unaltered at 2.6–2.7 ppm. So, considering that the expected conformation of the ligand arranges the two methyl groups (Fig. 1a) in clearly different environments and that only one of them suffers an important change of this situation upon coordination, it seems likely that the down-field methyl signals found for the P*t*Bu$_2$Xyl complexes above 3 ppm are due to the methyl group that points towards the metal (Me* in Fig. 1a).

The ^{31}P nuclei of the coordinated PR$_2$Xyl ligands in complexes **3** and **4** resonate as pairs of doublets due to coupling with the silver isotopes ^{107}Ag and ^{109}Ag, with chemical shift values significantly higher than those observed for the aforementioned Cu(I) derivatives, namely 32.6 and 36.2 ppm for **3d** and **3e**, and 52.7 and 52.4 for **4d** and **4e**, respectively. For the sake of comparison, two gold(I) complexes of formula AuCl(PR$_2$Xyl), **5a** (R = *i*Pr) and **6a** (R = *t*Bu), were prepared from AuCl(THT) and the corresponding phosphane in dichloromethane solution. The ^{31}P nuclei in **5a** and **6a** were found to resonate at 52.1 and 69.4 ppm, respectively, *i.e.* at much higher frequencies than the related Ag(I) complexes. After calculating an average value, $\bar{\delta}$, for the δ (^{31}P) of the coordinated phosphines (Table 1 5th column) for each group 11 metal, one can roughly recognize the following trend: $\bar{\delta}$ (^{31}P-Cu) < $\bar{\delta}$ (^{31}P-Ag) < $\bar{\delta}$ (^{31}P-Au), with separations between the mid-values of *ca.* 15–18 ppm. Taking into account that in all cases the coordination mode is found (or expected, for Au(I)) to be terminal (*vide infra*), it seems reasonable that the main factor that influences these δ values resides in the nature of the M−P bond. In fact, the electronegativities of the three coinage metals follow this trend, χ(Cu) < χ(Ag) ≪ χ(Au), which might result in a corresponding decrease of electron-density around the phosphorus nucleus and concomitant increase of the chemical shifts. Table 1 summarizes the most relevant ^{31}P{^{1}H} NMR data of complexes **1**–**6**.Table 2

Single crystals suitable for X-ray diffraction analyses were obtained for complexes **1a-c** and **2a-c** by slow cooling of *n*-heptane solutions of the compounds from *ca.* 90 °C to the room temperature. On the other hand, for triflate and triflimidate derivatives slow diffusion of *n*-heptane into dichloromethane solutions of the compounds produced crystalline samples suitable for crystallography. ORTEP diagrams of the molecular structures of complexes **1a-c** (P*i*Pr$_2$Xyl adducts of copper(I) halides), **2a-c** (P*t*Bu$_2$Xyl adducts of copper(I) halides), **1-2d** (PR$_2$Xyl adducts of copper(I) triflate), **3-4d** and **3e** (PR$_2$Xyl adducts of silver(I) triflate and triflimidate), are depicted in Figs. 2, 3, 4, and 5, respectively. With the exception of **4e**, for which no suitable crystals could be obtained, X-ray structural information of complexes **1**–**4** revealed, in all cases, terminal coordination of the phosphines to doubly bridged bimetallic cores [M(μ-X)]$_2$ (M = Cu: X = Cl, Br, I, OTf; M = Ag: X = OTf, NTf$_2$). These consist of 4-membered rings, for X = halide, or 8-membered rings, for X = OTf or NTf$_2$, with μ-κ*O*:κ*O*' or *μ*-κ*N*:κ*O* coordination modes, respectively.

Complexes [Cu(μ-X)(PR$_2$Xyl)]$_2$, **1a-c** (R = *i*Pr) and **2a-c** (R = *t*Bu), belong to a well-known class of dimeric Cu(I) derivatives [34,35], in which the trigonal planar coordination of each metal center is constituted by two bridging halides and one terminal P ligand. Cu-P bond distances, which span from 2.1887(5) (**1a**) to 2.2679(8) (**2c**) Å, are slightly but clearly influenced by the steric demand of both R groups and halides. So, while maintaining the same R substituent at P, Cu—P bond distances increase in the order d_{CuP}(*n***a**) < d_{CuP}(*n***b**) < d_{CuP}(*n***c**) (R = *i*Pr, *t*Bu: *n* = **1**, **2**, respectively); correspondingly, for each pair of adducts with the same X, d_{CuP}(**1** *m*) < d_{CuP}(**2** *m*) (X = Cl, Br, I: *m* = **a**, **b**, **c**, respectively). As documented for previously reported complexes of this type [35], the CuXCu bond angles are dramatically affected by the bridging halide, with the smallest values, 66.7° and 64.6°, found for the iodide derivatives **1c** and **2c**, respectively. On the other hand, for chloride and bromide complexes, CuXCu angles span from 73.3° to 82.0°, with no apparent correlation with any other structural or chemical parameters.

The shortest Cu•••Cu separations, of *ca.* 2.85 and 2.78 Å, are associated to the iodide adducts **1c** and **2c**, respectively, and approximately equal the double of copper covalent radius, thus pointing to the existence of closed-shell d^{10}-d^{10} interactions, typically named "cuprophilic" in this context [36,37]. Short Cu•••Cu separations are also found in **1b** and **2a**, for which the presence of metal–metal bonds cannot strictly be ruled out without specific theoretical examination. Interestingly, both complexes have non-planar [Cu(μ-X)]$_2$ cores, with the four atoms occupying the vertexes of a digonal disphenoid, thus reducing the distance between the two metal atoms located at opposite sites. As far as the conformations adopted by the coordinated P ligands in this series of complexes are concerned, α values (see Fig. 1c) are found in the range 10-30°, significantly increased with respect to the *ca.* 0° expected for the free PR$_2$Xyl ligands. This indicates that, upon coordination, the aromatic ring is slightly rotated from its initial position (α ≈ 0), likely to minimize repulsions between the Me* fragment of the Xyl moiety (see Fig. 1a-b) and the [M(μ-X)]$_2$ core.

Structural features of Cu(I) and Ag(I) complexes **1-4d** and **3e**, whose corresponding relevant data are listed in Table 3, will be discussed together in view of the numerous analogies that they share. Coordination environments at the metal centers are constituted by one P and two O atoms (P, O, and N for **3e**), giving rise to severely distorted trigonal planar geometries, with OMO angles in the range 90-100° for the triflate derivatives and 80.9 for the triflimidate **3e**.

As mentioned above, the 8-membered ring motif is a shared characteristic of all these complexes, acting the OTf$^-$ or NTf$_2$ anions as bridging ligands with μ-κ*O*:κ*O*' or μ-κ*N*:κ*O* coordination modes, respectively. Similar arrangements are known for Ag(I) [38–41] and Cu(I) triflate complexes [42], but also, for example, for some olefin adducts of CuCF$_3$CO$_2$ reported by Pampaloni and coworkers in 2005 [43]. Except for **4d**, which possesses a C_i-like symmetry but rigorously lacks an inversion center, the other derivatives of this series have centrosymmetric structures. Consequently, as witnessed by the β values listed in Table 3, the planar coordination environments of the two metal centers are parallel or coincide (Figs. 5 and 6). The latter situation is only found in complex **2d** and, on the condition that the substituents at P are not considered, generates a mirror plane perpendicular to the Cu•••Cu axis, providing a C_{2h}-like symmetry for the [PCuOTf]$_2$ fragment (Fig. 4, bottom; Fig. 6, top).

The S-bonded CF$_3$ fragments occupy *pseudo*-equatorial positions in the triflate derivatives **1-4d**, with the less sterically demanding oxo substituents at the corresponding axial sites, whereas in the triflimidate complex **3e** the F$_3$C—S═O angles are approximately bisected by the ring mid-plane (Fig. 6, bottom). Compared to what found for halide complexes **1a-c** and **2a-c**, α values for coordinated PR$_2$Xyl ligands are slightly smaller (2 to 13° *vs* 12 to 29°), thus locating the two R substituents in *quasi*-symmetrical dispositions with respect to the xylyl

plane.

Conformational analyses and structural studies of 8-membered cycles [44] established the existence of many possible stereoisomers of comparable energy, identifying, for instance, the boat–chair (C_s) and the crown (D_{4d}) conformers as the most stable for cyclooctane and S_8 [45], respectively (Fig. 7). Complexes **1-4d** and **3e** show otherwise a clear preference, at least in the solid state, for twist-chair conformations (C_i). For comparison, a conformational classification covering 8-membered cyclic cores enclosed in copper complexes with bridging P(V) ligands was reported by Pérez *et al.* in 2005 [46].

We finally decided to explore the possibility of preparing dinuclear cationic complexes of Cu(I), $[Cu_2(\mu\text{-}X)(PR_2Xyl)_2]$, by halide abstraction from the neutral adducts $[CuX(PR_2Xyl)]_2$. So, equimolar amounts of complex **1a** and $NaBAr^F$ (BAr^{F-} = tetrakis[3,5-bis(trifluoromethyl) phenyl]borate) were reacted in dichloromethane at room temperature, yielding selectively a new complex, **7·BAr^F**, whose NMR spectra did not show relevant differences compared to complexes **1a-d** apart from the signals due to the counteranion.

The molecular structure of **7·BAr^F** in the solid state was ascertained by X-ray diffraction analyses, which surprisingly revealed that, in lieu of the expected mono-bridged dinuclear complex $[Cu_2(\mu\text{-}Cl)(Pi Pr_2Xyl)_2]^+$, the mononuclear cationic complex $[Cu(Pi Pr_2Xyl)_2]^+$ had formed. This outcome, along with the absence of any other by-products such as elemental Cu, seems to indicate that, upon reacting with the chloride abstractor, complex **1c** converts into the mono-bridged cationic complex $[Cu_2(\mu\text{-}Cl)(Pi Pr_2Xyl)_2]^+$, which rapidly decomposes into CuCl and **7**$^+$. This species was also smoothly generated as a triflate salt, **7·OTf**, by reacting CuOTf•0.5(toluene) and P*i*Pr$_2$Xyl in a 1:2 M ratio in toluene at room temperature. Structurally characterized complexes of this class, albeit not very common, have been known for some decades [47–52]. It is worth mentioning that, surely as a consequence of the increased steric demand of the P ligand, none of our attempts to synthesize analogous cationic complexes with P*t*Bu$_2$Xyl, as triflate or BAr^{F-} salts, was successful.

Crystalline samples of **7·OTf** were also analyzed by X-ray diffraction. Relevant structural data of both cationic complexes are listed in Table 4, while the X-ray molecular structure of **7**$^+$ in **7·OTf** is depicted in Fig. 8 along with Newman-like projections of the cationic complexes in **7·OTf** and **7·BAr^F**. Both of them show distorted linear coordination environments at the Cu(I) centers with almost identical PCuP bond angles and distances of *ca.* 168-169° and 2.24–2.23 Å, respectively. The latter values are in the same range as those found for the P*i*Pr$_2$Xyl halide adducts **1a-c**, and somehow higher than in the triflate derivative **1d**. As shown in Fig. 8 (right), staggered conformations are adopted by the Cu-bonded phosphine ligands. The corresponding CP1•••P2C dihedral angles angles span from 45 to 78° with larger deviations from the 60° of perfectly staggered conformations in the triflate derivative **7·OTf**, which is certainly a consequence of different anion-cation interactions within the lattice of the two ion-pairs. Combined contributions of steric repulsions between the different P-bonded groups and weak interactions involving the copper atom are responsible for the synclinal disposition of the two xylyl substituents, being the corresponding dihedral angles of approximately 78 and 68° in **7·OTf** and **7·BAr^F**, respectively. Noteworthy, in both cations the metal center is located in the cylindrical sector defined by the two P—C_{Xyl} bonds at approximately 0.2 Å from the P••••P line. Although the X-ray molecular structures of the C_1 cations **7**$^+$ do not rigorously have any symmetry elements, a C_2-like symmetry can easily be envisaged for both species, the corresponding two-fold rotation axis passing through the P•••P and C15•••C1 mid-points (Fig. 9) and deviated by *ca.* 14 and 5° from P1CuP2 plane in **7·OTf** and **7·BAr^F**, respectively.

4. Conclusions

The sterically demanding xylyl-substituted phosphanes, P*i*Pr$_2$Xyl and P*t*Bu$_2$Xyl, the latter reported here for the first time, form stable dinuclear adducts with copper(I) halides of the general formula $[Cu(\mu\text{-}X)(PR_2Xyl)]$ (X = Cl, Br, I; R = *i*Pr, *t*Bu), all of them showing planar or bent $[Cu(\mu\text{-}X)]_2$ cores in the solid state with variable Cu•••Cu distances, which reach the lowest values of *ca.* 2.8 Å in the iodide derivatives, hence considered as metal–metal bonded complexes. Homo-bimetallic species with terminally coordinated P*i*Pr$_2$Xyl and P*t*Bu$_2$Xyl ligands were also obtained starting from Cu(I) and Ag(I) triflates, and $AgNTf_2$, whose X-Ray molecular structure consist in 8-membered centrosymmetric cyclic motifs, with the anions in a κ^2-μ^2 coordination mode and the phosphane ligands completing the distorted trigonal planar coordination of the metal centers. Moreover, the two-coordinate cationic complexes $[Cu(Pi Pr_2Xyl)_2]^+$, **7**$^+$, have been obtained as triflate or BAr^{F-} salts, and show distorted linear coordination in the solid state, with bond angles of approximately 168-169° and C_2-like symmetry. In these cations, the phosphine ligands adopt staggered conformations with respect to the P•••P axis with synclinal dispositions of the xylyl groups.

CRediT authorship contribution statement

Manuel Vaz: Investigation. **Alberto Gobbo:** Investigation. **M. Trinidad Martín:** Investigation. **Práxedes Sánchez:** Investigation. **Eleuterio Álvarez:** Investigation, Formal analysis. **Riccardo Peloso:** Conceptualization, Supervision, Investigation, Formal analysis, Writing – original draft.

Declaration of Competing Interest

The authors declare that they have no known competing financial interests or personal relationships that could have appeared to influence the work reported in this paper.

Data availability

Links are in the article text

Acknowledgements

This research was funded by Ministerio de Ciencia e Innovación (MICINN/AEI/10.13039/ 501100011033/, "ERDF A way of making Europe", Grant CTQ2017-82893-C2-2-R, Grants CTQ2016-75193-P, PID2019-110856GA-I00, and PID2020-113797R) and Junta de Andalucía (Grants US126226, P20_00624, FR-4688).

Appendix A. Supplementary data

Supplementary data to this article can be found online at https://doi.org/10.1016/j.ica.2023.121623.

References

[1] M. Bochmann, Organometallics and Catalysis, Oxford University Press, Oxford, An Introduction, 2015.
[2] R.H. Crabtree, The Organometallic Chemistry of the Transition Metals, Wiley, Hoboken, 2014.
[3] J. Hartwig, Organotransition Metal Chemistry: From Bonding to Catalysis, University Science Books, Sausalito, 2010.
[4] C. Elschenbroich, A. Salzer, Organometallics: A Concise Introduction, (2nd ed.),, Wiley-VCH, Weinheim, 1992.
[5] W.H. Bernskoetter, C.K. Schauer, K.I. Goldberg, M. Brookhart, Science 326 (2009) 553.
[6] A.J. Burke, H.-J. Federsel, G.J. Hermann, J. Org. Chem. 2022 (1898) 87.
[7] S.G. Roseblade, A. Pfalz, Acc. Chem. Res. 40 (2007) 1402.
[8] T. Imamoto, K. Tamura, Z. Zhang, Y. Horiuchi, M. Sugiya, K. Yoshida, A. Yanagisawa, I.D. Gridnev, J. Am. Chem. Soc. 134 (2012) 1754.
[9] P.W.V. Leeuwen, P.C. Kamer, C. Claver, O. Pamies, M. Dieguez, Chem. Rev. 111 (2011) 2077.
[10] W.S. Knowles, R. Noyori, Acc. Chem. Res. 40 (2007) 1238.
[11] X.-F. Wu, X. Fang, L. Wu, R. Jacksell, H. Neumann, M. Beller, Acc. Chem. Res. 47 (2014) 1041.
[12] W.A. Herrmann, C. Brossmer, C.-P. Reisinger, T.H. Riermeier, K. Oefele, M. Beller, Chem. Eur. J. 3 (1997) 1357.

[13] A.F. Littke, G.C. Fu, Angew. Chem. Int. Ed. 41 (2002) 4176.
[14] J.P. Stambuli, S.R. Stauffer, K.H. Shaughnessy, J.F. Hartwig, J. Am. Chem. Soc. 123 (2001) 2677.
[15] J.F. Hartwig, Acc. Chem. Res. 41 (2008) 1534.
[16] D.S. Surry, S.L. Buchwald, Angew. Chem. Int. Ed. 47 (2008) 6338.
[17] R. Martin, S.L. Buchwald, Acc. Chem. Res. 41 (2008) 1461.
[18] D.S. Surry, S.L. Buchwald, Chem. Sci. 2 (2011) 27.
[19] C.A. Tolman, J. Am. Chem. Soc. 92 (1970) 2956.
[20] C.A. Tolman, W.C. Seidel, L.W. Gosser, J. Am. Chem. Soc. 96 (1974) 53.
[21] C.A. Tolman, Chem. Rev. 77 (1977) 313.
[22] J. Campos, E. Carmona, Organometallics 34 (2015) 2212.
[23] J. Campos, R. Peloso, E. Carmona, Angew. Chem. Int. Ed. 51 (2012) 8255.
[24] J. Campos, L. Ortega-Moreno, S. Conejero, R. Peloso, J. López-Serrano, C. Maya, E. Carmona, Chem. Eur. J. 21 (2015) 8883.
[25] M.M. Alcaide, P. Sánchez, E. Álvarez, C. Maya, J. López-Serrano, R. Peloso, Dalton Trans. 51 (2022) 5777.
[26] A.J. Cheney, B.L. Shaw, J. Chem. Soc., Dalton Trans. 754 (1972).
[27] H.V. Rasika Dias, C. Dash, M. Yousufuddin, M.A. Celik, G. Frenking, Inorg. Chem. 50 (2011) 4253.
[28] M.A. Celik, C. Dash, V.A.K. Adiraju, A. Das, M. Yousufuddin, G. Frenking, H. V. Rasika Dias, Inorg. Chem. 52 (2013) 729.
[29] Á. Beltrán, I. Gata, C. Maya, J. Avó, J.C. Lima, C.A.T. Laia, R. Peloso, M. Outis, M. C. Nicasio, Inorg. Chem. 59 (2020) 10894.
[30] T. Nickel, K.-R. Pörschke, R. Goddard, C. Krüger, Inorg. Chem. 31 (1992) 4428.
[31] N.A. Yakelis, R.G. Bergman, Organometallics 24 (2005) 3579.
[32] Modification of the procedure described for similar phosphines in: S. Maehara, H. Iwazaki, WO 2003066643 A1. Japan: Hokko Chemical Industry; **2003**.
[33] M. Marín, J.J. Moreno, C. Navarro-Gilabert, E. Álvarez, C. Maya, R. Peloso, M. C. Nicasio, E. Carmona, Chem. Eur. J. 25 (2019) 260.
[34] K.G. Caulton, G. Davies, E.M. Holt, Polyhedron 9 (1990) 2319.
[35] G.L. Soloveichik, O. Eisenstein, J.T. Poulton, W.E. Streib, J.C. Huffman, K. G. Caulton, Inorg. Chem. 31 (1992) 3306.
[36] N.V.S. Harisomayajula, S. Makovetskyi, Y.-C. Tsai, Chem. Eur. J. 25 (2019) 8936.
[37] S. Sculfort, P. Braunstein, Chem. Soc. Rev. 40 (2011) 2741.
[38] K.M.A. Malik, P.D. Newman, Dalton Trans. (2003) 3516.
[39] R. Terroba, M.B. Hursthouse, M. Laguna, A. Mendia, Polyhedron 18 (1999) 807.
[40] M. Bardaji, O. Crespo, A. Laguna, A.K. Fischer, Inorg. Chim. Acta 304 (2000) 7.
[41] M.H. Garcia, P. Florindo, M.F.M. Piedade, M.T. Duarte, Polyhedron 28 (2009) 239.
[42] J.C. Tendyck, H. Klocker, L. Schurmann, E.-U. Wurthwein, A. Hepp, M. Layh, W. Uhl, J. Org. Chem. 85 (2000) 14315.
[43] G. Pampaloni, C. Graiff, R. Peloso, A. Tiripicchio, Organometallics 24 (2005) 819.
[44] H.B. Hendrickson, J. Am. Chem. Soc. 89 (1967) 7047.
[45] P. Coppens, Y.W. Yang, R.H. Blessing, W.F. Cooper, F.K. Larsen, J. Am. Chem. Soc. 99 (1977) 760.
[46] J. Pérez, L. García, M. Kessler, K. Nolsøe, E. Pérez, J.L. Serrano, J.F. Martínez, R. Carrascosa, Inorg. Chim. Acta 358 (2005) 2432.
[47] E.W. Ainscough, A.M. Brodie, A.K. Burrell, J.V. Hanna, P.C. Healy, J.M. Waters, Inorg. Chem. 38 (1999) 20.
[48] B.K. Najafabadia, J.F. Corrigan, Dalton Trans. 44 (2015) 14235.
[49] R. J. Davidson 1, E. W. Ainscough, A. M. Brodie, G. H. Freeman, G. B. Jameson, *Polyhedron* **2016**, *119*, 584.
[50] P.D. Akrivos, P.P. Karagiannidis, C.P. Raptopoulou, A. Terzis, S. Stoyanov, Inorg. Chem. 35 (1996) 4082.
[51] A. Ziółkowska, S. Brauer, Ł. Ponikiewski, Z. Anorg, Allg. Chem. 645 (2019) 949.
[52] P. Mehlmann, C. Muck-Lichtenfeld, T. Tan, F. Dielmann, Chem. Eur. J. 23 (2017) 5929.